Application of Printable Electronics for LCD Manufacturing: Printing of TFT Gate Layers and Pillar Spacers

D. B. van Dam, M. P. J. Peeters, C. J. Curling, R. Schroeders, and M. A. Verschuuren*
Philips Research, Eindhoven, The Netherlands
** now at Plastic Logic Limited, Cambridge, United Kingdom*

Abstract

Applying printing technology to manufacturing of electronics promises significant cost reductions. However, many interesting applications require increased accuracy of graphical printing hardware, excellent electronic functionality of the printed materials, and also introduce complicated 'ink'-substrate interactions.

In this paper we present results of ink jet printing gate metal lines of thin-film transistors (TFTs) on a liquid crystal display's (LCD) active plate. The major components of this study are 1) the formulation of metal precursor inks that have good electrical properties, 2) the printing and layer formation of the materials, and 3) the manufacturing and characterisation of TFT arrays with a printed gate and storage capacitor lines. In addition, we show results on printed spacers for LCDs.

We demonstrate printed gate lines (50 µm wide and 250 nm thick) with a resistivity of around 3 µΩ·cm, cured at 350 °C. During layer formation, Rayleigh-type instabilities were prevented and favourable layer thickness profiles have been obtained by tuning the printing frequency, evaporation rate of the solvent, and type of metal colloids. Fabricated TFTs have similar characteristics as those obtained with conventional methods and materials (on-off ratio $>10^6$ and a mobility around 0.5 cm^2/Vs).

Introduction

Motivation

Industrial manufacturing of LCD back planes is performed using technology that originates from the IC industry. These photolithographic-based processes have a resolution sufficient for AMLCD requirements. While in the IC world the primary development has been in the decrease of feature size, in the LCD world the main development has been in the increase of substrate size. Currently, substrates of about 2.1 m × 1.8 m are planned to be processed in generation 7 AMLCD factories.

The use of (vacuum) equipment for these large substrates significantly increases the capital investment needed in a factory. It can be envisioned that next generation factories may therefore not be economical. This could open up possibilities for printing-based processes, if reliability and accuracy are sufficient. Compared to photolithography, printing processes for making structures on the active plate lead to less process steps, less materials, less capital expenditure and less clean-room space.

The work on printed pillar spacers has both a quality and cost aspect. The positioning of the spacers – made possible with ink jet printing – can increase the uniformity in the pixel area. This improves the optical display quality compared to the conventional randomly applied ball spacers. Compared to photolithographically-defined pillar spacers, printed pillar spacers have a potential cost advantage.

Research Focus

We choose an active plate design suitable for a VGA LCD-TV application, because of the relatively large pixels and importance of cost for this product. We concentrated our research efforts in three areas: materials, printing, and TFT design. The materials work was aimed at finding ink-jet printable materials with good electrical functionality, which also yield the required layer thickness of about 200 nm. In this paper we report results on ink-jet printable nano-particle silver suspensions, a route that was also explored in e.g. Ref. 1. In the printing part we mainly concentrated on the fluid-solid interactions. Printing for displays requires different substrates and inks compared to graphical printing, which induces new issues. The design and manufacturing of TFTs was aimed at optimizing the structure for ease of printability. In addition, we had a separate effort in showing the initial feasibility of printed spacers.

Other Work on Printing for AMLCDs

One of the earlier studies of using printing technology for TFT manufacturing was via gravure offset printing.[2] By printing an optical mask on top of a sheet resist layer, the gate structure was defined. In a more recent study,[3] ink-jet printed wax was used for applying a patterned etch resist layer. The printing of materials with direct electrical functionality was performed by Furusawa *et al.*,[4] where bus electrodes for plasma panels were manufactured by ink jet printing. The printing of spacer-like structures was introduced in Ref. 5.

Experimental

Commercially-available water-based nano-particle silver was obtained from Merck (Silber kolloid reinst, 101507) and Nippon-Paint (a dispersion containing 17 wt.% silver). The average particle size of the Merck silver colloids is around 30 nm, that of the Nippon-Paint varied somewhat but is within the range from 1 to 5 nm. The silver dispersion was first diluted in water, after which a 2 wt.% methyltri-methoxysilane (MTMS) solution was added. A typical ink had a silver content of 8 wt.% and an MTMS content of 0.4 wt.%, giving about 10 vol.% of the fully condensed CH_3-$SiO_{3/2}$ in the final layer. The viscosity of the Nippon-Paint based ink was 4.1 mPa·s at a shear rate of 10 s^{-1}, while the Merck-based ink had a viscosity of 1.2 mPa·s. The surface tension of the ink was measured and was shown not to change significantly as a result of the MTMS addition. For manufacturing of spacers, we used the acrylic monomer hexanediol diacrylate (HDDA) to which a small amount of sensitizer was added (~ 0.01 wt.% Irgacure 651). The viscosity of this fluid was 4.6 mPa·s.

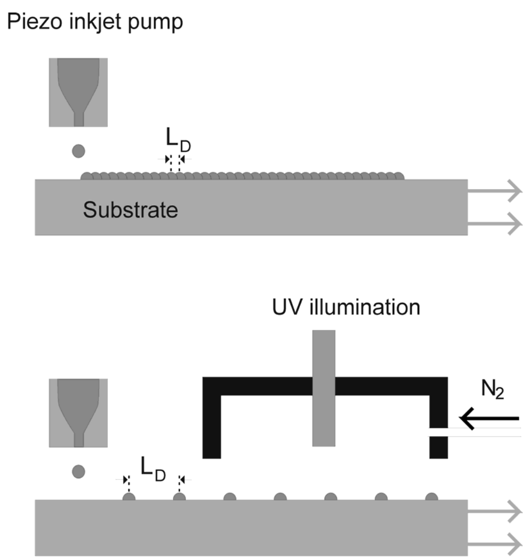

Figure 1. Experimental set-up for printing experiments of silver (top) and spacers (bottom). L_D is the distance between printed droplets and V_S is the substrate velocity.

The materials were printed using a single-nozzle ink jet head obtained from Microdrop GmbH (Norderstedt, Germany). The ink jet head contains a glass capillary without an internal restriction, and has a 30 μm inner diameter nozzle. The piezo element has a cylindrical shape, and encloses the glass capillary. An XY stage (Schaad, Switzerland) with 1 μm positioning accuracy carries the glass substrate. Figure 1 schematically shows the set-up. It also shows an extension to this set-up that was made for the manufacturing of spacers. The printed monomer droplets pass a UV lamp (from EFOS, Toronto, Canada; type Acticure, maximum intensity at 365 nm), which illuminates the spacers when they pass through an enclosure that is flushed with nitrogen. In this way the spacer material is cured quickly after printing, before significant evaporation has taken place.

For printing gate patterns, we aimed at printing on flat glass substrates without any supporting structures to assist correct ink flow. This was done to keep the process simple and prevent the necessity of extra process steps. In order to prevent excessive spreading of the ink on the substrate and to improve stability, we uniformly changed the surface energy of the glass substrates. 5x6 inch glass plates were modified by vapour priming using methylaminopropyldimethoxysilane for printing gate lines. In that way an advancing contact angle of 70 ± 5 deg. and a receding contact angle of 20 ± 5 deg. could be achieved for water. The substrates contained all photolithographic alignment marks and lead-outs, but were without the central active area array of the gate lines and storage capacitor lines, which were to be printed. The glass plates for the spacers were covered by ITO and were 5 × 5 cm in size. Surface modification was performed by vapour priming using 1H-1H-2H-2Hperfluorodecyltriethoxy-silane, giving a contact angle for the HDDA monomer of 55 ± 5 deg. Both types of glass plates were cleaned thoroughly including a UV-ozone step before vapour priming.

After printing of the nano-particle silver, the substrates were cured in an oven for about 60 minutes. Further manufacturing of the bottom-gate thin film transistors was performed in a research line for TFT array processing in the Philips Research Laboratories in Redhill, UK. Although the multitude of processes on this line prevented similar yield as in a factory, the process was comparable with an industrial manufacturing process.

Results

Materials

The addition of the small amount of MTMS to the ink gave good conductivity, prevented instability during curing, and gave sufficient adhesion of the silver on the glass. In this way we achieved stable silver layers and printed patterns, while conductivity was sufficient.

During curing the stabilizing organic components in the ink are removed. Figure 2 shows resistivity as a function of curing temperature of both spin-coated layers and printed lines (referred to as traces), for different amounts of added MTMS. It shows that resistivities < 5 μΩ·cm – being fairly close to the bulk resistivity of silver (1.6 μΩ·cm) – can be achieved. This conductivity is sufficient for our application.

Printing of Silver Lines in AMLCDs

Four basic issues were encountered during printing. These were 1) the droplet formation process and size of the generated droplets, 2) the impact process of the droplets on the substrate, 3) the stability of the fluid structure on the substrate, and 4) the drying process of the fluid structure.

Droplet formation and size is strongly dependent on the print head and driving pulse. Because we used a simplified single-nozzle print head, we did not pay much attention to this issue. Generated droplets of silver ink were 35 - 40 µm in diameter. The HDDA droplets had a diameter of about 20 µm.

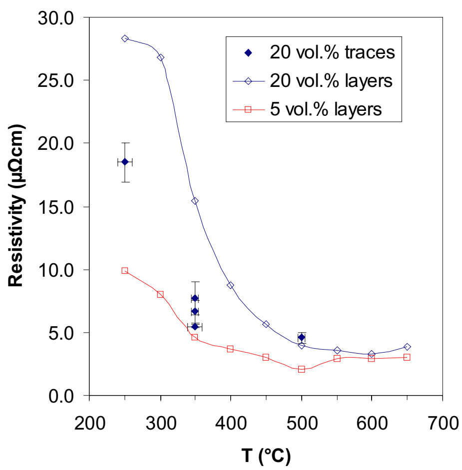

Figure 2. Resistivity of the inkjet printed traces - based on Nippon Paint silver dispersion - as a function of curing temperature, compared to spin coated layers containing different quantities of MTMS. The curing time was 30 - 60 minutes in an oven in air.

The dynamics of the impact process was studied using a separate set-up with which the impact process of a single droplet on a substrate can be studied. Although in a practical printing process part of the droplet impacts on the previously printed fluid, we found that single-droplet impact gives a good prediction of the line width. Figure 3 shows pictures that were typically recorded. In figure 4 we plotted the maximum radius increase of the printed droplets – with respect to the initial radius – as a function of the Weber number $We = \rho U_0^2 D_0/\sigma$ (ρ is the fluid density, U_0 the droplet's impact velocity, D_0 the droplets' diameter in free flight, and σ the fluid's surface tension). One main result was that up to a Weber of about 10, the static contact angle determined the final radius. For larger Weber numbers, the droplets spread beyond their equilibrium contact angle. Further details of this study can be found in Ref. [6].

When a line of fluid was deposited on the substrate, fluid instabilities were observed. These were comparable to observations in previous papers.[7,8] It was found in these studies that the stability of a line of fluid on a substrate depends on the mobility of the contact line, which in our case is determined by the actual contact angle compared to the equilibrium advancing and receding contact angles.

In our study instabilities appeared as depicted in figure 5. By measuring the distance between the blobs of fluid, an average wavelength related to the instability could be determined. It was found that the wavelength of the instability increased when the substrate velocity V_S and the printing frequency decreased, keeping the distance between the droplets L_D constant. Below a certain threshold for the substrate velocity, stable lines could be printed. In our experiments, this threshold was about 0.5 mm/s, while L_D typically was 60 µm for a droplet diameter of 40 µm.

Figure 6 shows the wavelength of the instability versus the estimated length of the line over which the fluid has not dried yet. We see that when the naturally-occurring wavelength λ becomes about equal to the length of the non-dried line length L, the instabilities disappear and the line becomes stable. L is defined as $h \cdot V_S/e_v$, where h is the initial wet layer thickness and e_v is the average evaporation velocity. In this way, a stable region can be identified.

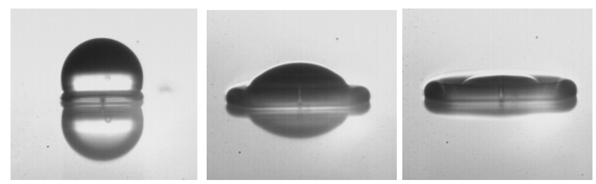

Figure 3. Successive stages of an impacting droplet, with mirror image from the glass substrate. In this example, the initial droplet diameter is 70 µm, the time interval between the pictures is 6 µs.

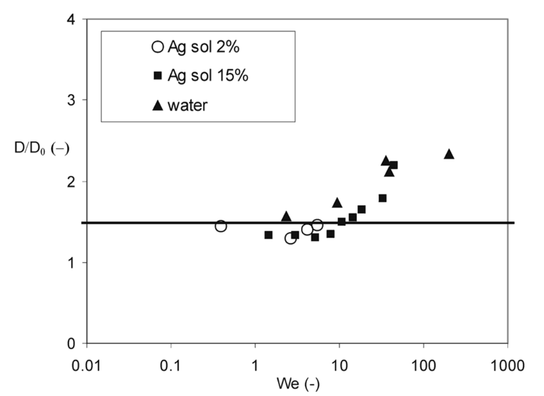

Figure 4. Maximum sessile droplet diameter D after impact normalised by the initial diameter D_0 as a function of Weber number We.

An extreme way of preventing instabilities is to allow each droplet to dry before the next droplet is printed, or to print non-connected droplets and fill in the gaps during a second run. In both cases the process speed will be lowered. An alternative approach to obtain stable lines appears to be to increase the impact speed so that droplets spread beyond their advancing contact angle. In combination with a large contact line hysteresis (i.e. low receding contact angle), this will prevent movement of the contact line. As we used the ink jet head at a Weber number of about 2, the value of this approach was not verified experimentally.

During the drying process of the fluid, convective transport of silver particles takes place within the fluid. This effect was quantitatively explained by Deegan.[9] He optically measured the amount of mass that accumulated near the contact line. These measurements agreed with a model in which the contact line was assumed to remain pinned, fluid flow was assumed to be inviscid, and the fluid surface was assumed to have the shape of a spherical cap.

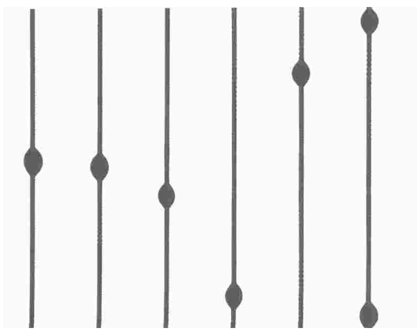

Figure 5. Example of instabilities encountered for printed silver lines on glass (line width is 50 μm).

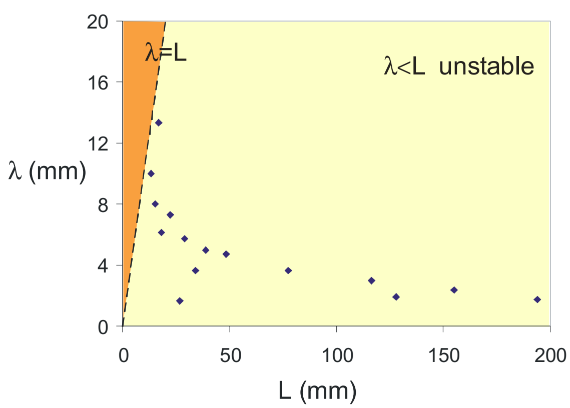

Figure 6. Observed instability wavelength λ and non-dry line length L. A region with unstable lines (λ<L) can be identified.

For the small colloids in our silver dispersions and the relatively small dimensions of the printed patterns, we found diffusion of silver particles to be important as well. Such diffusion establishes a flow of colloids from the edge of the droplet – where the concentration is higher – towards the center, thus counteracting the convective mass transport. In order to understand the drying process, we solved the convection-diffusion equation for both a radial (droplets) and 2D (lines) geometry, under the same assumption as Deegan for the shape of the droplet. By measuring the viscosity of the fluid as a function of concentration, we determined a critical concentration above which the fluid does not flow anymore and mass transport stops. More details on the modelling can be found in Ref. [10].

Based on the modelling it was found that for water-based suspensions, a diffusion-dominated drying regime can be obtained for the Nippon Paint silver with its small particles. In this drying regime, convection-induced concentration gradients during drying are effectively opposed by diffusive mass transport. As a result, the dried layer thickness will mimic the initial wet layer thickness, and a convex layer thickness will result. Actually this is the preferred shape for TFT gate layers, as it will give good step coverage by the overlaying gate dielectric layer. This behaviour was confirmed in experiments. Figure 7 shows typical examples of the printed layer thickness distribution for silver with large particles (top figure) and small particles (bottom figure). It shows that for the larger Merck particles – where convective mass transport towards the edge is dominant – a non-favourable layer thickness distribution resulted. The smaller Nippon Paint particles showed the convex layer thickness distribution.

After curing, the final lines had dimensions of 50 μm width and approximately 250 nm thickness (by using ink jet heads with a 40 μm inner diameter nozzle, also 80 μm wide lines were made). This gives a sheet resistivity of about 0.2 Ω/sq., which is sufficient for this LCD-TV application.

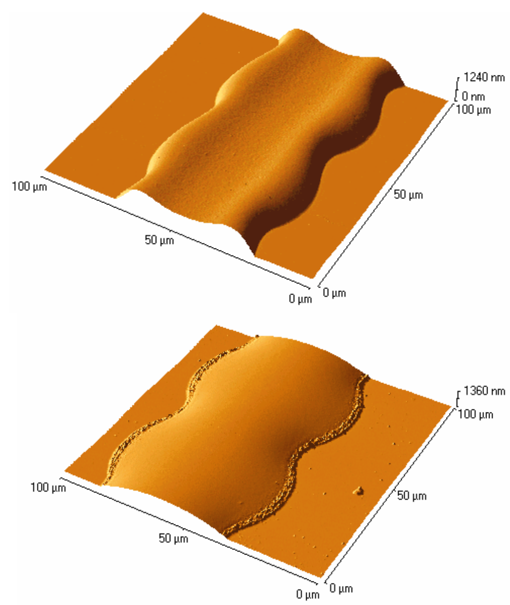

Figure 7. AFM measurement of printed layer thickness distribution after drying and before curing.

TFT Design and Manufacturing

Our TFT design[11] was adjusted for easy of printability, having e.g. a relatively simple gate layer (unidirectional line) and being relatively tolerant of alignment errors. Figure 8 shows an example of a part-processed TFT array with a printed gate and storage capacitor lines. The printed lines showed some raggedness near the edge, in which the individual droplets can be recognized. This is caused by the applied hydrophobicity of the substrate. The printed lines are typically 50 µm wide, with a variation of ± 5 µm due to the edge raggedness. In the example in figure 8, the gate lines would preferably be 20% wider in order to correct for alignment errors elsewhere on the display, as the gate line should overlap with the whole of the semiconductor islands. In the example of figure 8, the pixel ITO and top insulator layers are not shown.

The dimension of an RGB pixel in the present design is about 800 × 800 µm, corresponding to a VGA TV design. We were able to print 200 lines of 9 cm length without any line irregularity (see figures 5 and 8 for examples of such irregularities). A clean environment and careful substrate handling were found to be essential to achieve this goal.

The silicon nitride gate dielectric and hydrogenated amorphous silicon semiconductor layer were both deposited by PECVD and patterned using 'conventional' photolithography. The source-drain metal was sputtered and again photolithographically patterned.

We made TFTs having similar electrical characteristics to those obtained with conventional methods and materials: on-off ratio $>10^6$ and a mobility around 0.5 cm^2/Vs. Figure 9 shows an example of the I-V characteristics of the TFTs.

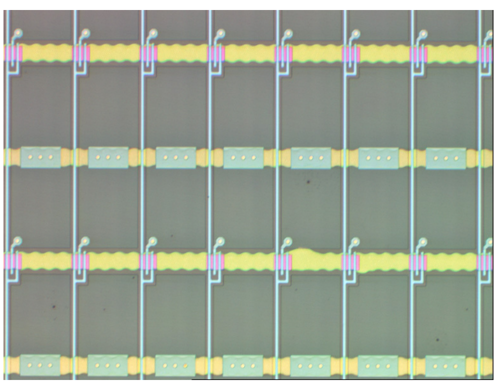

Figure 8. Part-processed TFT array with printed gate and storage capacitor lines. One irregularity is visible on the lower printed (horizontal) gate line.

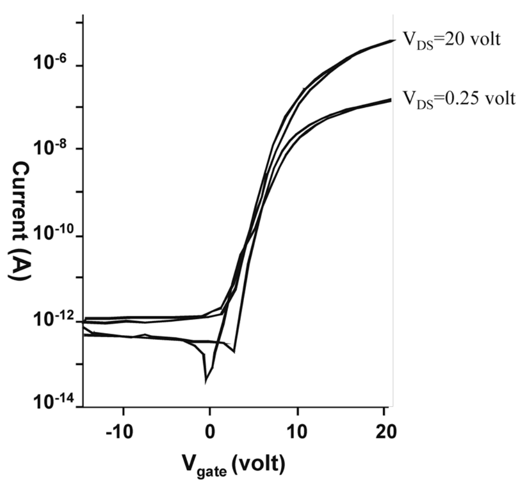

Figure 9. I-V characteristics of a TFT with a printed gate.

Spacers

With the surface modification, we were able to print LCD spacers that were about 35 µm in diameter and had a thickness of 8 µm. These were printed in a regular grid (see figure 10). After printing, the spacers were put in UV-ozone in order to remove the fluoro silane monolayer coating. This did not significantly diminish the thickness of the (organic) spacers. For cleaning the substrates with the spacers, we used cleaning steps with soap, demineralised water, and iso-propyl alcohol. Because of the relatively poor adhesion, ultrasonic cleaning steps tended to remove some of the spacers.

After cleaning, a polyimide alignment layer was applied by spin coating, followed by rubbing. The rubbing was antiparallel. After application of glue around the edges, a second glass plate is place on top of the substrate with the spacers. As the cell gap uniformity is the first critical test for the uniformity of the spacers, we evaluated two cells to evaluate the cell gap uniformity. It was found that the cell gap was uniform within 4%, which is already close to a typically required specification of 3%.

One cell was filled with liquid crystal, for which we used a liquid crystal mixture with parallel alignment and a birefringence Δn of 0.0993. The pretilt of the alignment layer was about 1 deg. We determined the uniformity of the cell's light transmission. The "one-pixel" cell showed a reasonably uniform intensity over the display area.

Figure 11 shows the 50 x 50 mm cell driven by a block pulse with 20 V RMS at 900 Hz. The black spots in the center of the spacers are caused by the Hertzian contact between the spacer and the upper glass plate, in combination with the crossed polarisers which extinguish the light. At low driving voltages, a shadow is visible behind the spacers. This is possibly the result of the rubbing of the alignment layer after application of the spacers: the spacers are thought to cause a small distortion in the alignment layer.

Drop-on-demand industrial printing takes place using a multi-nozzle ink jet head. The droplet diameters, droplet volume variations, and placement accuracy of graphical print heads is usually not sufficient for the printing of spacers. The latest print heads from Spectra (Lebanon (NH), USA) – developed for printing of PLED materials for display mass manufacturing – shows sufficiently small droplet volume variation and good placement accuracy.[12]

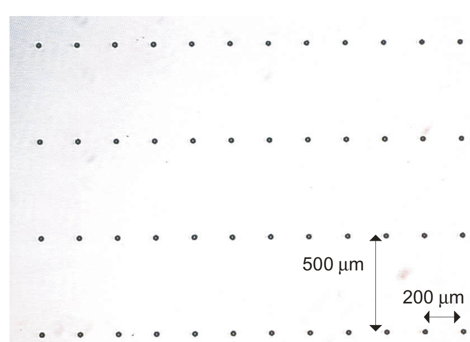

Figure 10. Pattern of printed spacers.

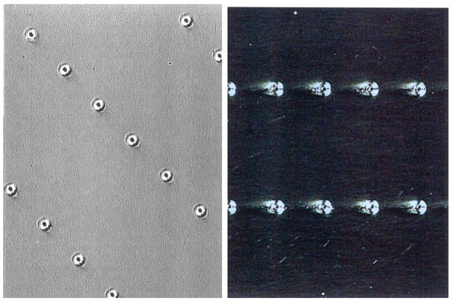

Figure 11. LC cell with crossed polarisers at 20 V driving voltage (left, rubbing direction makes 45° angle with polarisers) and 0 V (right, rubbing direction makes 0° angle with one of the polarisers). Distances between spacers are equal as in figure 10.

Conclusions

In this paper we describe an initial feasibility study of ink jet printed gate metal lines and printed pillar spacers for LCDs. This manufacturing method can be expected to yield cost advantages compared to manufacturing by vacuum processes in combination with photolithographic patterning.

We showed that using a printable nano-particle silver dispersion, TFT arrays with acceptable electrical characteristics can be made. By tuning ink properties and applying a uniform substrate energy modification, stable lines with favourable cross-sections were made. These lines had sufficient conductivity for LCD-TV applications.

This study also gives an encouraging confirmation of applying ink jet printing for pillar spacer manufacturing in LCDs.

Acknowledgements

We wish to thank Julie Ross for her help in TFT array manufacturing, Gerda van de Spijker for manufacturing the LCD cells with printed spacers, and Leo van den Besselaar and Michel Bruyninckx for their effort in building the printing set-up.

References

1. J. B. Szczech, C. M. Megaridis, D. R. Gamota, J. Zhang, Manufacture of Microelectronic Circuitry by Drop-On-Demand Dispensing of Nano-Particle Liquid Suspensions, MRS Spring Meeting Proceedings 624, 23 (2000).
2. Y. Mikami, Y. Nagae, Y. Mori, K. Kuwabara, T. Saito, H. Hayama, H. Asada, Y. Akimoto, M. Kobayashi, S. Okazaki, K. Asaka, H. Matsui, K. Nakaura, and E. Kaneko, A New Patterning Process Concept for Large-Area Transistor Circuit Fabrication Without using an Optical Mask Aligner, IEEE Transactions on Electron Devices 41, 306 (1994).
3. W. S. Wong, S. E. Ready, J.-P. Lu, R. A. Street, Hydrogenated Amorphous Silicon Thin-Film Transistor Arrays Fabricated by Digital Lithography, IEEE Electron Device Letters 24, 577 (2003).
4. M. Furusawa, T. Hashimoto, M. Ishida, T. Shimoda, H. Hasei, T. Hirai, H. Kiguchi, H. Aruga, M. Oda, N. Saito, H. Iwashige, N. Abe, S. Fukuta, and K. Betsui, "Inkjet-Printed Bus and Address Electrodes for Plasma Display, Proceedings SID (2002).
5. M. Grove, D. Hayes, R. Cox, D. Wallace, J. Caruso, M. Hampden-Smith, T. Kodas, K. Kunze, A. Ludviksson, S. Pennino and D. Skamser, Color Flat Panel Manufacturing Using Ink Jet Technology_Proceedings Display Works '99, San Jose, Feb., 1999.
6. D. B. van Dam and C. Le Clerc, Impact of an Ink-Jet Printed Droplet on a Solid Substrate, Phys. Fluids 16, 3403 (2004).
7. S. Schiaffino and A. A. Sonin, Formation and Stability of liquid and molten beads on a solid surface, J. Fluid Mech. 343, 95 (1997).
8. S. H. Davis, Moving contact lines and rivulet instabilities. Part 1. The static rivulet, J. Fluid Mech. 98, 225 (1980).
9. R. D. Deegan, Contact line deposits in an evaporating drop, Physical Review E 62, 756 (2000).
10. D. B. van Dam, Layer Thickness Distribution of Thin-Film Ink-Jet Printed Structures, proceedings XXI ICTAM04 Congress, 15-21 August 2004, Warsaw, Poland.
11. S. C. Deane and C.J. Curling, Printable thin film transistor designs and method of manufacture, patent GB0105145.
12. M. Fleuster, M. Klein, P. V. Roosmalen, A.d. Wit, H. Schwab, Mass Manufacturing of Full Color Passive-Matrix and Active-Matrix PLED Displays, proceedings SID (2004).

Biographies

Dirkjan van Dam holds a M.Sc. degree in Applied Physics (1993) and a Ph.D. degree in Applied Geophysics (1999), both from Delft University of Technology. He joined Philips Research in 1999. His research interests are in fluid mechanics and mechanics of granular materials. Since 1999, he has worked at Philips Research on spin coating and ink jet printing of electronic materials for flat displays, with a current emphasis on PLED display manufacturing.

Mart Peeters graduated from the Eindhoven University of Technology in 1989 (Chemical Engineering), followed by a PhD on the preparation and characterization of molecular sieves in 1993. After a post-doc at the University of Nijmegen (NMR spectroscopy) he joined Philips Research in 1995. The main field of research was on sol-gel chemistry (coatings) and polymer electrolytes. In 2004 he moved to the Central Development department of Philips Lighting.

Catherine J. Curling graduated with a BSc(Hons) Physics degree from Bristol University in 1985, before joining Philips Research Redhill. She has over 15 years experience of developing new process technologies from their innovative inception through to successful industrial commercialisation. Her technology remits have included AMLCDs, fingerprint and image sensors (both optical and X-ray). In 2004, she joined the Management Team at Plastic Logic Limited, Cambridge, as Chief Technology Officer.

Richard Schroeders holds a B.Sc. degree in Applied Physics (1998) from Fontys University Eindhoven. He joined Philips Research in 1999. His research interest are in ink jet printing of bio materials and polymer layer thickness measurements for PLED-TV. He also worked on spin coating and micro-contact printing.

Marc Verschuuren holds a B.Sc. degree in Chemical Engineering (2001) in materials engineering, from Fontys University Eindhoven. Since then, he has worked on sol-gel chemistry for ink-jet printing purposes, and soft lithography of sol-gel materials for optical applications.